Tuberous Sclerosis Complex Suppression in Cerebellar Development and Medulloblastoma: Separate Regulation of Mammalian Target of Rapamycin Activity and p27^{Kip1} Localization

Bobby Bhatia,[1] Paul A. Northcott,[2] Dolores Hambardzumyan,[1] Baskaran Govindarajan,[3] Daniel J. Brat,[3] Jack L. Arbiser,[3] Eric C. Holland,[1] Michael D. Taylor,[2] and Anna Marie Kenney[1]

[1]Department of Cancer Biology and Genetics, Memorial Sloan-Kettering Cancer Center, New York, New York; [2]Division of Neurosurgery, The Hospital for Sick Children, The University of Toronto, Toronto, Ontario, Canada; and [3]Department of Dermatology, Emory School of Medicine, Atlanta, Georgia

Abstract

During development, proliferation of cerebellar granule neuron precursors (CGNP), candidate cells-of-origin for the pediatric brain tumor medulloblastoma, requires signaling by Sonic hedgehog (Shh) and insulin-like growth factor (IGF), the pathways of which are also implicated in medulloblastoma. One of the consequences of IGF signaling is inactivation of the mammalian target of rapamycin (mTOR)–suppressing tuberous sclerosis complex (TSC), comprised of TSC1 and TSC2, leading to increased mRNA translation. We show that mice, in which TSC function is impaired, display increased mTOR pathway activation, enhanced CGNP proliferation, glycogen synthase kinase-3α/β (GSK-3α/β) inactivation, and cytoplasmic localization of the cyclin-dependent kinase inhibitor p27^{Kip1}, which has been proposed to cause its inactivation or gain of oncogenic functions. We observed the same characteristics in wild-type primary cultures of CGNPs in which TSC1 and/or TSC2 were knocked down, and in mouse medulloblastomas induced by ectopic Shh pathway activation. Moreover, Shh-induced mouse medulloblastomas manifested Akt-mediated TSC2 inactivation, and the mutant TSC2 allele synergized with aberrant Shh signaling to increase medulloblastoma incidence in mice. Driving exogenous TSC2 expression in Shh-induced medulloblastoma cells corrected p27^{Kip1} localization and reduced proliferation. GSK-3α/β inactivation in the tumors *in vivo* and in primary CGNP cultures was mTOR-dependent, whereas p27^{Kip1} cytoplasmic localization was regulated upstream of mTOR by TSC2. These results indicate that a balance between Shh mitogenic signaling and TSC function regulating new protein synthesis and cyclin-dependent kinase inhibition is essential for the normal development and prevention of tumor formation or expansion. [Cancer Res 2009;69(18):7224–34]

Introduction

Medulloblastoma is the most common malignant solid pediatric tumor. These tumors arise in young children in the cerebellum, a dorsal brain structure. Current treatment regimens for medulloblastoma cause developmental, behavioral, and cognitive disturbances in long-term survivors. These devastating side effects underscore the need to understand the basic mechanisms underlying medulloblastoma initiation, expansion, and recurrence, so that novel treatments can be developed which specifically target tumor cells without damaging the developing brain.

Cerebellar granule neuron precursors (CGNP), a proposed cell-of-origin for medulloblastomas (1), proliferate rapidly during a transient postnatal expansion phase in the cerebellar external granule layer a (EGLa). CGNPs become postmitotic in the EGLb, then migrate inward and terminally differentiate in the internal granule layer (IGL). The CGNP expansion phase requires signaling by Sonic hedgehog (Shh) and insulin-like growth factor (IGF; refs. 2, 3). Aberrant Shh pathway activation is found in sporadic medulloblastomas and in Gorlin's syndrome, in which patients carry mutations or deletions in the Patched (*Ptc*) gene (4, 5), a key inhibitory component of the Shh receptor complex.

IGF pathway activity is also found in medulloblastomas in both mice and humans (6, 7). IGF signaling activates the kinase mammalian target of rapamycin (mTOR), which promotes mRNA translation. Growth factors activate mTOR by turning off the tuberous sclerosis complex (TSC), composed of TSC1 (hamartin) and TSC2 (tuberin), which normally keeps mTOR in check (8, 9). TSC1 stabilizes TSC2 protein; TSC2's GTPase-activating protein function inhibits mTOR. TSC2 overexpression results in decreased mTOR activity, whereas abrogating TSC1 or TSC2 function results in increased mTOR activity and excessive cell growth. Conversely, TSC1 or TSC2 overexpression impedes cell cycle progression (10, 11). TSC2 positively regulates the cyclin-dependent kinase inhibitor p27^{Kip1} by preventing its degradation (12) and promoting its nuclear localization (13). Akt-mediated TSC2 phosphorylation impairs its ability to inhibit mTOR/S6K, but does not affect TSC2-mediated control of p27^{Kip1}, indicating that TSC2's regulation of mTOR and p27^{Kip1} are separable functions.

In the developing cerebellum, p27^{Kip1} is expressed in the EGLb, the molecular layer, and the IGL (14, 15). In adult cerebella, p27^{Kip1} is expressed in the cells of the IGL. p27^{Kip1} heterozygous or null mice possess cerebella that are larger than those of wild-type mice (14). Importantly, loss of p27^{Kip1} in Patched+/− mice increased the incidence of medulloblastoma (16). CGNPs prepared from p27^{Kip1}-deficient mice show enhanced proliferation compared with CGNPs from wild-type mice (14). The Roussel and Eisenman groups have shown an antagonistic relationship between p27^{Kip1} and the Shh target N-myc during cerebellar development (17, 18). N-myc and D-type cyclins are destabilized by glycogen synthase kinase (GSK)-3α/β activity (2, 19).

We used transgenic mice constitutively expressing a dominant negative TSC2 allele (20) to investigate whether TSC inhibition

Note: Supplementary data for this article are available at Cancer Research Online (http://cancerres.aacrjournals.org/).

Requests for reprints: Anna Marie Kenney, Department of Cancer Biology and Genetics, Memorial Sloan Kettering Cancer Center, New York, NY 10021. Phone: 646-888-2051; Fax: 646-422-0231; E-mail: kenneya@mskcc.org.

doi:10.1158/0008-5472.CAN-09-1299

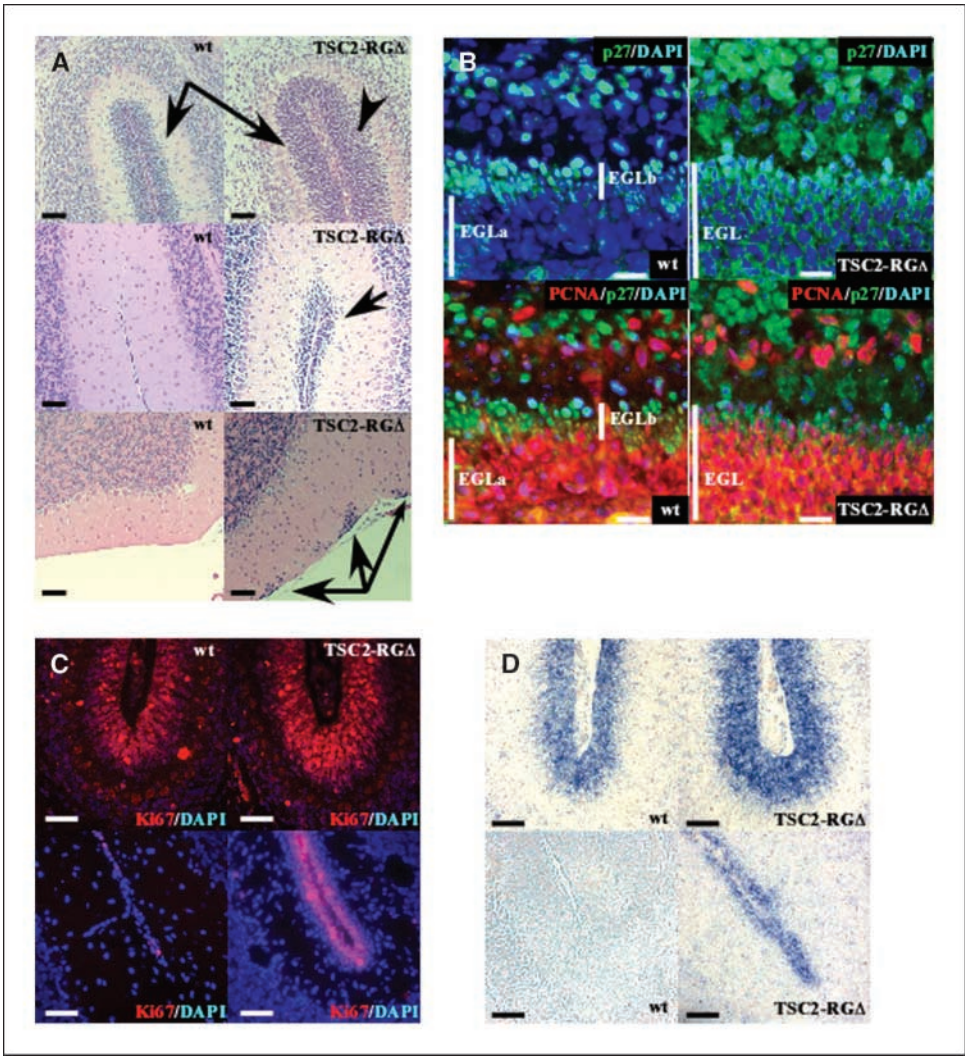

Figure 1. TSC2 inactivation leads to abnormal cerebellar development and p27Kip1 misregulation. *A,* TSC2 inactivation leads to abnormal cerebellar development in mice. *Top row,* sagittal sections of H&E-stained postnatal day 7 wild-type or TSC2-RGΔ cerebella. *Arrows,* molecular layer, compressed in the mutant mice. *Arrowhead,* expanded EGL in TSC2-RGΔ. *Middle row,* sagittal sections of H&E-stained postnatal day 15 wild-type and TSC2-RGΔ cerebella. *Arrow,* retained EGL in TSC2-RGΔ cerebellum. *Bottom row,* sagittal sections of H&E-stained adult cerebellum. *Arrow,* rests, clusters of cells which have failed to migrate to the IGL. *B,* p27Kip1 is mislocalized in TSC-inactive cerebella. Immunofluorescence analysis of p27Kip1 levels and localization in postnatal day 7 wild-type and TSC2-RGΔ sagittal sections shows that wild-type mice have nuclear p27Kip1 (*green*) in postmitotic region EGLb, whereas TSC2-RGΔ mice have cytoplasmic localization of p27Kip1 throughout the EGL (*top row*). PCNA shows proliferating cells in EGLa (*red*). Nuclei costained with 4′,6-diamidino-2-phenylindole (*DAPI; blue*). *White line,* the entire EGL (TSC2-RGΔ) and EGLa/EGLb (wild-type). Magnification, ×80. *C,* the expanded and retained EGL in TSC2-RGΔ cerebella contains proliferating cells as indicated by immunofluorescence staining for the proliferation marker Ki67 (*red*). Ki67 staining is localized in the EGL of postnatal days 7 and 15 cerebella. TSC2-RGΔ mice have increased Ki67 (*right*) compared with wild-type (*left*) in postnatal day 7 (*top row*) and postnatal day 15 (*bottom row*). Ki67 (*red*) was costained with DAPI (*blue*). Magnification, ×40. *D,* the expanded and retained EGL in TSC2-RGΔ cerebella contains proliferating cells, as indicated by *in situ* hybridization for cyclin D2. Cyclin D2 can be detected in the EGL of wild-type and TSC2-RGΔ mice at postnatal day 7, but by postnatal day 15 (*bottom*), only the mutant mice still have cyclin D2–expressing cells in the EGL. Magnification, ×40. *Bars, A* (*top* and *middle row*), *C* and *D,* 16 μm; *A* (*bottom row*), 32 μm; *B,* 8 μm.

plays a role(s) in CGNP expansion and medulloblastoma. These mice possess clusters of granule neurons that fail to migrate to the IGL, and they have cerebellar development abnormalities consistent with enhanced CGNP proliferation. CGNPs from these mice had mTOR signaling pathway activity resembling that of mouse Shh-driven medulloblastomas, including enhanced rpS6 phosphorylation, inactivation of GSK-3α/β, and cytoplasmically localized $p27^{Kip1}$. In Shh-driven medulloblastoma cells, introduction of wild-type TSC2 caused $p27^{Kip1}$ to go to the nucleus and reduced proliferation. Interestingly, $p27^{Kip1}$ was not relocalized to the nucleus by treatment with mTOR inhibitors, indicating that its subcellular localization is regulated by TSC2 upstream of mTOR. Our results suggest that loss of TSC activity can synergize with Shh signaling to alter cerebellar development and enhance medulloblastoma expansion via combined effects on mTOR activation, GSK-3α/β inactivation, and $p27^{Kip1}$ cytoplasmic localization.

Materials and Methods

Mice. *TSC2-RGΔ*, $Ptc^{+/-}$, and *NeuroD2-SmoA1* mice were generated and maintained on a C57/BL6 background. Mice were managed according to the Memorial Sloan Kettering Cancer Center policies described in A.M. Kenney's Institutional Animal Care and Use Committee–approved protocol. *NeuroD2-SmoA1* mice were provided by Dr. Jim Olson (Fred Hutchinson

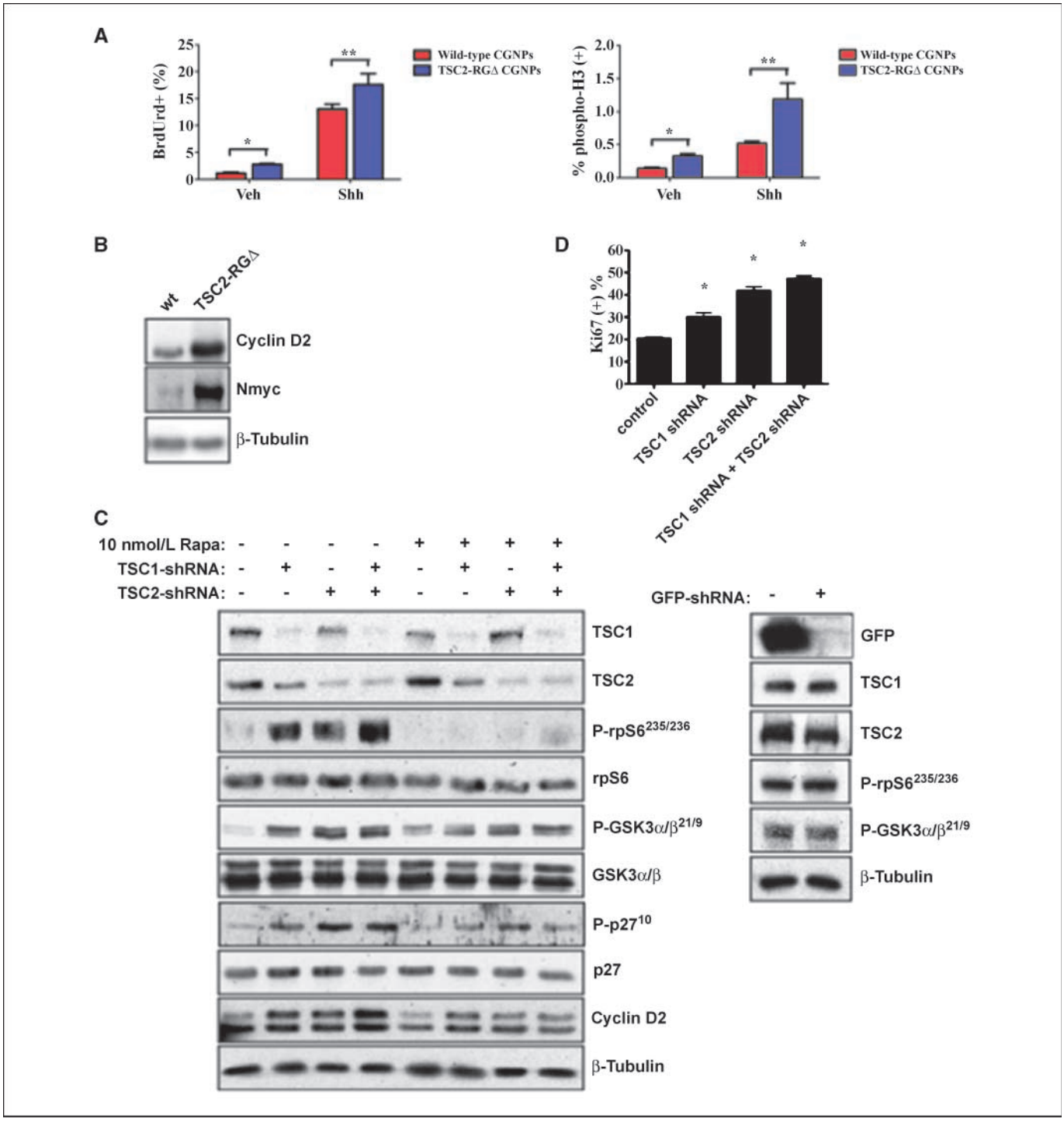

Figure 2. TSC inactivation increases the basal proliferative capacity of CGNPs through increased mTOR signaling and inactivating phosphorylation of p27Kip1 and GSK-3α/β. *A,* quantification of BrdUrd incorporation in wild-type and TSC2-RGΔ CGNPs treated with Shh or vehicle alone (*left*). Vehicle-treated mutant CGNPs have significantly higher levels of BrdUrd incorporation than wild-type CGNPs (*, $P = 0.0004$). In the presence of Shh, TSC2-RGΔ CGNP BrdUrd incorporation is significantly greater than that of Shh-treated wild-type CGNPs (**, $P = 0.0245$). Two-tailed *t* tests were used to test significance. *Right,* quantification of staining for the mitotic marker phosphorylated histone H3 in wild-type and TSC2-RGΔ CGNPs treated with Shh or Shh vehicle alone. TSC2-RGΔ CGNPs have increased levels of phosphorylated histone H3 in comparison with wild-type CGNPs even in the absence of Shh (*, $P = 0.0021$). Levels of phosphorylated histone H3 are significantly increased in mutant CGNPs in the presence of Shh (**, $P = 0.0108$). Two-tailed *t* tests were used to test significance. *B,* Western blot shows that TSC2-RGΔ CGNPs have higher endogenous levels of cyclin D2 and N-myc in comparison with wild-type freshly isolated CGNPs. β-Tubulin was used as a loading control. Representative data from four wild-type postnatal day 4/5 mice and four TSC2-RGΔ postnatal day 4/5 mice. *C,* Western blot analysis of wild-type Shh-treated CGNPs infected with TSC shRNA lentiviruses. Pooled TSC shRNA lentiviruses increased the phosphorylation of rpS6, phosphorylation of GSK-3α/β, mislocalized p27Kip1, and proliferation due to TSC knockdown. Short-term treatment with mTOR inhibitor rapamycin blocks S6 phosphorylation but does not significantly affect phosphorylated p27Kip1 and cyclin D2 levels. GFP shRNA lentiviruses were used as controls to knock down GFP in CGNPs derived from Math1-GFP mice. Protein levels from TSC1, TSC2, phosphorylated rpS6, and phosphorylated GSK-3α/β protein levels were unaffected. *D,* knockdown of TSC significantly increases CGNP proliferation (*, $P < 0.0001$). Ki67 staining was quantified using automated detection and scoring. One-way ANOVA test was used to test significance.

Cancer Center, Seattle, WA). *Math1-GFP* mice were provided by Jane Johnson (UT Southwestern, Dallas, TX).

Cell culture and lentivirus production. For CGNP culture, postnatal day 4 or 5 mice were used as previously described (21). The CGNPs were treated with Shh (1 μg/mL; R&D Systems) to promote proliferation. Where indicated, rapamycin (Calbiochem) and wortmannin (Calbiochem) were used at 10 nmol/L for 6 h. Proteasome inhibitor lactacystin (Calbiochem) was used at 10 nmol/L for 4 h.

Pzp53med cells (kindly provided by Dr. Matt Scott, Stanford University, Stanford, CA) were grown in DMEM containing 10% fetal bovine serum and 1% penicillin/streptomycin (B. Bhatia and A.M. Kenney). Pzp53med cells were transfected with either pcDNA3.1-TSC2 or pRK-TSC2 (both plasmids kindly provided by Dr. Pier Paolo Pandolfi, Harvard Medical School, Boston, MA) using Fugene 6. Cells were fixed after 48 h of posttransfection.

TSC1, TSC2, and green fluorescent protein (GFP) short hairpin RNA (shRNA) lentiviral constructs were obtained from Sigma. Four constructs of each were transfected into a mouse macrophage cell line or GFP-expressing cells, and Western blotting was used to determine which shRNAs effectively and specifically targeted TSC1, TSC2, and GFP (data not shown; Fig. 2). Effective constructs were used to prepare lentiviruses.

Western blot analysis. Protein extraction and Western blotting were carried out as previously described (21). Primary antibodies were TSC1 (Cell Signaling), TSC2 (Cell Signaling), GSK-3α/β (Upstate Biotechnology), p-GSK-3α/β$^{Ser21/9}$ (Cell Signaling), cyclin D2 (Santa Cruz Biotechnology), N-myc (Santa Cruz Biotechnology), p27^{Kip1} (BD Transduction Laboratories), p-p27^{Ser10} (Santa Cruz Biotechnology), ribosomal protein S6 (Cell Signaling), p-rpS6$^{Ser235/236}$ (Cell Signaling), p-mTOR^{Ser2481} (Cell Signaling), mTOR (Cell Signaling), proliferating cell nuclear antigen (Calbiochem), GFP (Calbiochem), vascular endothelial growth factor (Santa Cruz Biotechnology) and β-tubulin (Sigma). Horseradish peroxidase–conjugated secondary antibodies were goat anti-rabbit IgG (H + L) at 1:3,000 (Pierce Labs) and donkey anti-mouse IgG (H + L) at 1:5,000 (The Jackson Laboratory).

Immunohistochemistry and *in situ* hybridization. Postnatal day 7 brains were fixed in 4% paraformaldehyde at 4°C, processed for paraffin-embedding, and sectioned at 10 μm. Immunohistochemistry and RNA *in situ* hybridization were performed using standard methods. Immunohistochemistry and *in situ* hybridization (cyclin D2) were performed on sagittal sections. Detailed protocols are available at the Memorial Sloan-Kettering Cancer Center web site.[4]

Immunocytochemistry. CGNPs and Pzp53med cells were fixed in 4% paraformaldehyde for 10 min. Postnatal days 7 and 15, adult brains, and tumors were fixed in 4% paraformaldehyde at 4°C, processed for paraffin-embedding, and sectioned at 10 μm. Immunocytochemistry and bromodeoxyuridine (BrdUrd) incorporation detection were carried out as described (21). Primary antibodies are listed above, with the exception of BrdUrd (BD Transduction Laboratories), Ki67 (Vector Labs), p-H3^{Ser10} (Cell Signaling), GFAP (Cell Signaling), and Bmi1 (Upstate Biotechnology). Secondary antibodies were AlexaFluor 555 goat anti-rabbit IgG (H + L) at 1:1,000 (Invitrogen) and AlexaFluor 488 goat anti-mouse IgG (H + L) at 1:1,000 (Invitrogen). BrdUrd incorporation was measured using the MetaMorph imaging system.

Results

TSC inactivation leads to abnormal cerebellar development and p27^{Kip1} mislocalization. We wished to determine how the TSC complex might be regulated in the context of normal and oncogenic Shh signaling. However, TSC1-null and TSC2-null mice die *in utero*; TSC1$^{+/-}$ and TSC2$^{+/-}$ mice are not reported to have cerebellar abnormalities (22), suggesting that the remaining TSC alleles are sufficient to support TSC function in the developing brain in those mice. Therefore, we made use of mice transgenic for a *TSC2* allele lacking Rheb-GTPase–activating protein function (20), termed *TSC2-RGΔ*. The cerebellum of these mice were reported to contain "rests," which may represent failed preneoplastic lesions (23, 24), but they do not develop medulloblastomas (20), consistent with the observation that humans with TSC mutations are not predisposed to medulloblastoma.

We evaluated *TSC2-RGΔ* mice at three stages of cerebellar development: postnatal day 7, postnatal day 15, and in adults. RT-PCR analysis confirmed the expression of the dominant negative TSC2 transgene (Supplementary Fig. S1*A*). *TSC2-RGΔ* mice have a significantly thicker EGL compared with wild-type controls in postnatal day 7 (Fig. 1*A*, *arrow*, quantification shown in Supplementary Fig. S1*B*). At postnatal day 15, when CGNPs from wild-type mice have left the EGL, *TSC2-RGΔ* mice still possessed an EGL several cells thick. Rests were observed at the cerebellar surface in *TSC2-RGΔ* adult cerebella as previously reported (20).

We focused on postnatal day 7, the stage of development at which CGNP proliferation is at its peak, to identify mechanisms through which TSC inactivation contributes to CGNP proliferation. The cyclin-dependent kinase (CDK) inhibitor p27^{Kip1} is an essential negative regulator of CGNP proliferation (14). In cell lines, p27^{Kip1} has been reported to interact with TSC2, which retains p27^{Kip1} in the nucleus (10, 13). When we analyzed p27^{Kip1} protein in wild-type and *TSC2-RGΔ* cerebella, we detected nuclear p27^{Kip1} in postnatal day 7 wild-type mice (Fig. 1*B*) in the EGLb, where CGNPs are leaving the cell cycle. In contrast, p27^{Kip1} was distributed throughout the EGL of *TSC2-RGΔ* mice. This p27^{Kip1} was entirely located in the cytoplasm, where other studies have proposed that it becomes degraded or takes on inappropriate functions (25–27).

The *TSC2-RGΔ* cerebella display widespread rpS6 phosphorylation in the mitotic region EGLa and differentiated region IGL (Supplementary Fig. S1*C*), indicating up-regulation of mTOR activity. Consistent with impaired cell cycle exit, the EGL of *TSC2-RGΔ* mice had increased Ki67 levels (Fig. 1*C*) at postnatal days 7 and 15. Next, we examined the expression of *cyclin D2*, an effector of N-myc activity in the developing mouse cerebellum (28). The expanded EGL at postnatal day 7 and the retained EGL at postnatal day 15 of *TSC2-RGΔ* cerebella have increased *cyclin D2* expression (Fig. 1*D*). These findings suggest that TSC inactivation leads to abnormal cerebellar development due to increased proliferation in the EGL, associated with mislocalized p27^{Kip1}.

TSC inactivation increases the basal proliferative capacity of CGNPs. Addition of Shh to the medium permits the proliferation of CGNP primary cultures (29–31) although exogenous IGF is required for their survival (32, 33). Shh treatment elicited a significantly higher level of proliferation in *TSC2-RGΔ* CGNPs as compared with wild-type CGNPs (Fig. 2*A*) as determined by BrdUrd incorporation and histone H3 phosphorylation. In comparison with wild-type CGNPs, *TSC2-RGΔ* CGNPs have increased endogenous levels of N-myc and cyclin D2 (Fig. 2*B*). These results indicate that *TSC2-RGΔ* CGNPs have an increased intrinsic capacity for proliferation and that TSC inhibition may cooperate with Shh signaling to further enhance CGNP proliferation.

Because Shh-mediated medulloblastomas and *TSC2-RGΔ* mice might have mutations in other pathways that result in p27^{Kip1} dysregulation and GSK-3α/β inactivation, we wished to determine how acute shRNA-mediated disruption of TSC signaling in wild-type CGNPs affects p27^{Kip1} and GSK-3α/β. As shown in Fig. 2*C*, infection with shRNA-carrying lentiviruses targeting TSC1 and/or TSC2 effectively reduced their protein levels in infected CGNPs. GFP knockdown in CGNPs derived from Math-GFP mice did not affect mTOR pathway activity (Fig. 2*C*).

[4] http://www.mskcc.org/mskcc/html/77387.cfm

TSC knockdown resulted in increased rpS6 phosphorylation. Compared with control-infected CGNPs, there was an increase of phosphorylated $p27^{Kip1}$ (Ser10) levels following TSC knockdown. Phosphorylation at this site promotes $p27^{Kip1}$ export to the cytoplasm (34, 35). Treatment with mTOR inhibitor rapamycin blocked S6 phosphorylation, but only modestly changed phosphorylated $p27^{Kip1}$ levels compared with control CGNPs, suggesting that regulation of $p27^{Kip1}$ in CGNPs depends on the TSC, and is not downstream of mTOR. These results contrast with a recent study carried out in cell lines, wherein $p27^{Kip1}$ localization was found to be regulated downstream of mTOR (36). We also observed increased GSK-3α/β phosphorylation following TSC knockdown, which was reduced by rapamycin treatment. Cyclin D2, a CGNP proliferation marker, and Ki67 immunostaining show that proliferation is increased by TSC knockdown (Fig. 2*C* and *D*).

TSC2 inactivation increases Shh-mediated medulloblastoma incidence. *TSC2-RGΔ* CGNPs showed increased phosphorylation of the serine/threonine kinase mTOR and rpS6 (Fig. 3*A*), consistent with maintained mTOR activation, in comparison with wild-type

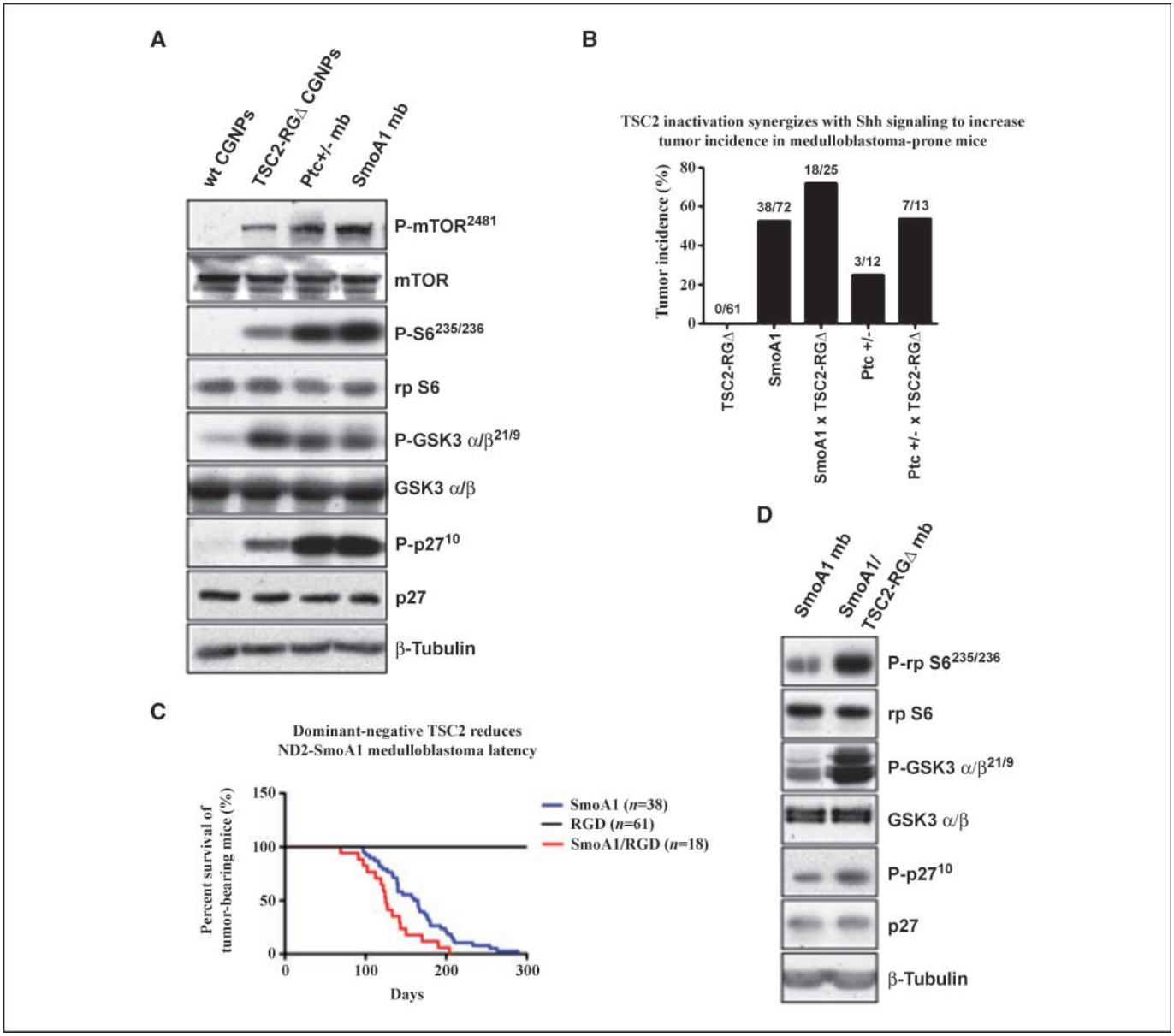

Figure 3. TSC2 inactivation in mice leads to p27Kip1 mislocalization, GSK-3α/β destabilization, and decreased survival latency. *A,* protein lysates extracted from age-matched postnatal days 4/5 wild-type and TSC2-RGΔ CGNPs, and medulloblastomas from Patched heterozygote ($Ptc^{+/-}$) and NeuroD2-smoothened mutant (SmoA1) mice were used for Western blot analyses of the indicated proteins. Data representative of four wild-type mice, four TSC2-RGΔ mice, three $Ptc^{+/-}$ medulloblastomas, and six SmoA1 medulloblastomas. *B,* medulloblastoma incidence in NeuroD2-SmoA1 and $Ptc^{+/-}$ mice in the presence or absence of TSC2-RGΔ allele. Increased tumor incidence suggests that inactivation of the TSC can synergize with oncogenic Shh signaling. *C,* Kaplan-Meier survival curve indicates survival latency in SmoA1 tumor-bearing mice in the presence or absence of TSC2-RGΔ allele. TSC2-RGΔ mice were crossed into the SmoA1 line. Tumors arising in the SmoA1/TSC2-RGΔ mice (*red*) have shorter latency than SmoA1 alone (*blue*). Survival curves are significantly different using Gehan-Breslow-Wilcoxon ($P = 0.0084$) and Mantel-Cox ($P = 0.0063$) tests. *D,* TSC2 inactivation in SmoA1 medulloblastoma enhances mTOR signaling, GSK-3α/β inactivation, and p27Kip1 phosphorylation. Protein lysates extracted from tumors of SmoA1 and SmoA1/TSC2-RGΔ mice were used for Western blot analyses of the indicated proteins. Data representative of three SmoA1 medulloblastomas and three SmoA1/TSC2-RGΔ medulloblastomas.

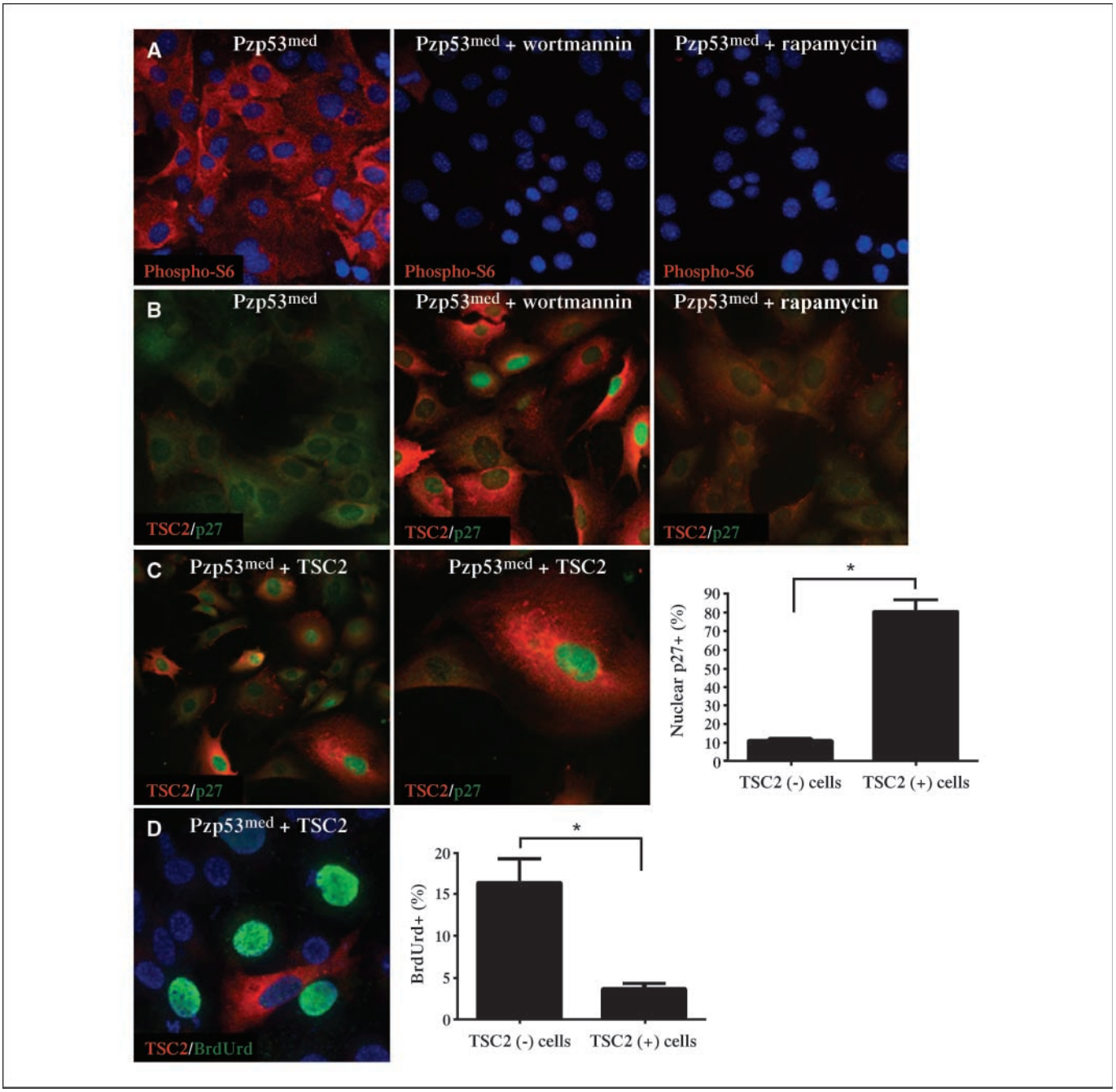

Figure 4. TSC inactivation and p27Kip1 dysregulation in medulloblastoma cells are associated with increased proliferation. *A,* under normal conditions, Pzp53med cells have phosphorylated ribosomal S6 protein. Cells treated with 10 nmol/L of phosphoinositide-3-kinase inhibitor wortmannin or 10 nmol/L of mTOR inhibitor rapamycin for 8 h shut down the levels of phosphorylated S6. Cells were immunostained for phosphorylated rpS6 (*red*) and costained for DAPI (*blue*). Magnification, ×40. *B,* under normal conditions, Pzp53med cells have barely detectable TSC2 and p27Kip1 (*left*). Akt inhibition with 10 nmol/L of wortmannin for 8 h rescued TSC2 and nuclear-localized p27Kip1 (*middle*). However, mTOR inhibition by 10 nmol/L of rapamycin for 8 h did not rescue either of these two proteins (*right*). TSC2 (*red*) and p27Kip1 (*green*) were costained. Magnification, ×40. *C,* ectopic TSC2 expression retains nuclear p27Kip1 in medulloblastoma cells. Nuclear p27Kip1 can be easily detected in cells transfected with exogenous TSC2 (*left* and *middle*). High-power image shows striking contrast in p27Kip1 localization between a TSC2-transfected cell and an untransfected neighboring cell (*middle*). Magnification, ×40 (*left*) and ×63 (*right*). TSC2 (*red*) and p27Kip1 (*green*) were costained. *Right,* automated quantification of TSC2 and p27Kip1 immunostaining. The vast majority of TSC2-positive cells have nuclear p27 (*, $P < 0.0001$). Two-tailed *t* tests were used to test for significance. *D,* TSC2-expressing cells have reduced immunostaining for BrdUrd incorporation (*left*). TSC2 (*red*) positive cells are BrdUrd-negative (*green*). Cells were costained with DAPI (*blue*). *Right,* results from an automated quantification of TSC2 and BrdUrd immunostaining. TSC2-positive cells have significantly reduced proliferation (*, $P = 0.0003$). Two-tailed *t* tests were used to test significance.

CGNPs. Interestingly, the *TSC2-RGΔ* cerebella also had increased levels of phosphorylated GSK-3α/β and Ser10 phosphorylated $p27^{Kip1}$ (26, 34, 35). Likewise, we detected phosphorylated mTOR, rpS6, GSK-3α/β, and $p27^{Kip1}$ (Ser10) in medulloblastomas from $Ptc^{+/-}$ mice and *SmoA1* mice, which express an activated mutant allele of the Shh receptor component, Smoothened (37). Thus, the signaling abnormalities in *TSC2-RGΔ* cerebella are also present in mouse medulloblastomas. Taken together, our results indicate that

TSC inactivation in *TSC2-RGΔ* mice and Shh-induced mouse medulloblastomas could promote cell cycle progression as a result of increased mTOR-mediated protein synthesis, mislocalized $p27^{Kip1}$, and inactivated GSK-3α/β, which is predicted to result in N-myc and D-type cyclin stabilization (2, 19).

We next introduced the *TSC2-RGΔ* transgene into mice with a heterozygous null mutation for *Ptc* and the *NeuroD2-SmoA1* mice. Dominant negative TSC2 increased medulloblastoma incidence in both $Ptc^{+/-}$ (53.8% versus 25%) and *SmoA1* (72% versus 52.8%) mice (Fig. 3*B*). Also, TSC2 inactivation in *SmoA1* tumor-bearing mice

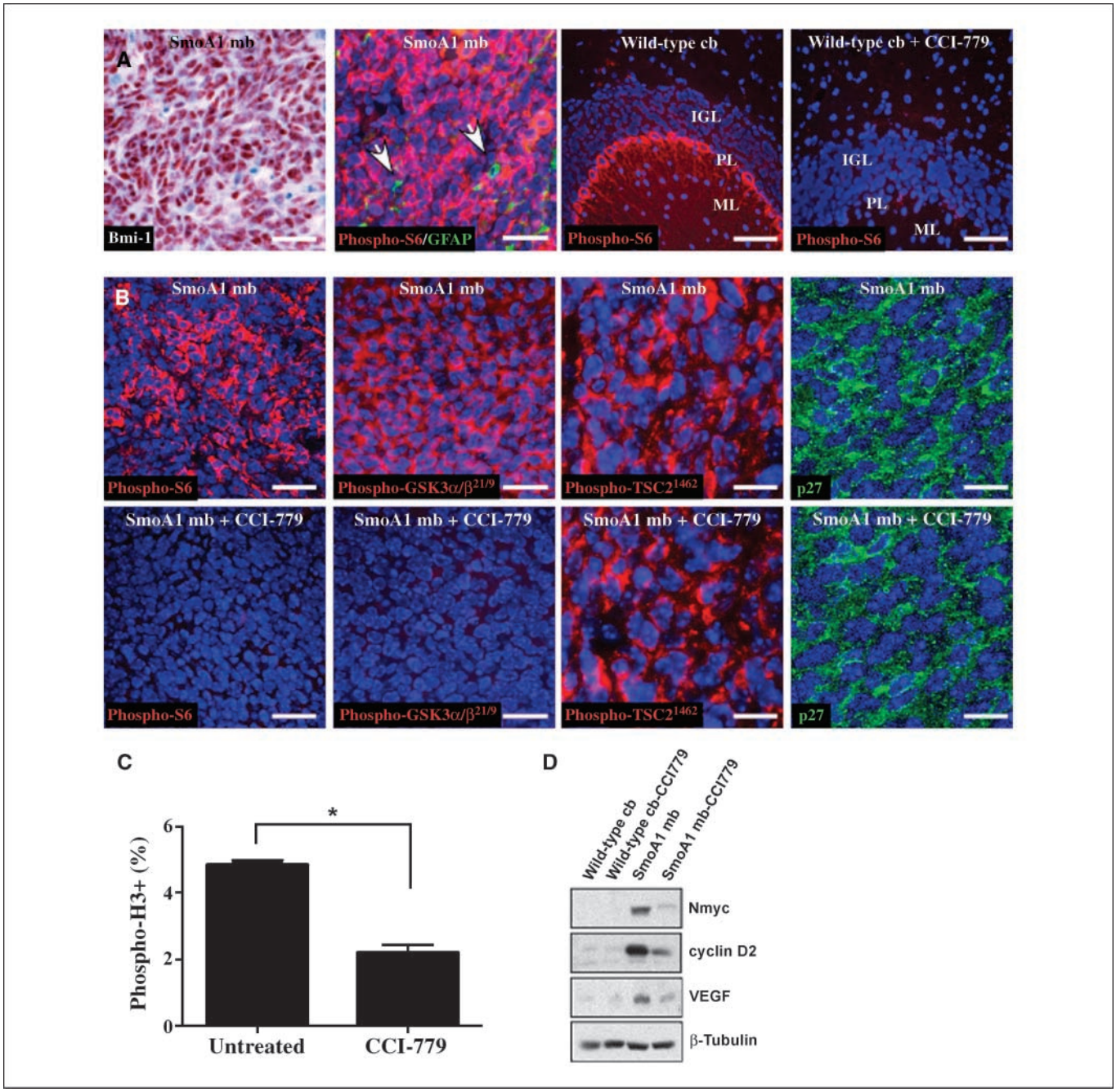

Figure 5. TSC2 phosphorylation, p27Kip1 localization, and GSK-3α/β phosphorylation in Shh-mediated medulloblastoma. *A,* SmoA1 medulloblastoma tumor cells have robust Bmi 1 (DAB staining), phosphorylated S6 protein (*red*), and little GFAP (*green*). Only Purkinje neurons (*PL*) of wild-type adult cerebella have phosphorylated rpS6. Representative image from a wild-type mouse treated with mTOR inhibitor CCI-779 shows loss of phosphorylated rpS6 in Purkinje neurons, indicating that this drug crosses the blood-brain barrier. Magnification, ×40. *B,* SmoA1 medulloblastoma untreated (*top row*) or treated (*bottom row*) with CCI-779 for 10 d. Immunostaining for phosphorylated S6 (*red; first column*) serves as a read-out for mTOR activity. Phosphorylated GSK-3α/β (*red; second column*) is affected by mTOR inhibition. Inactivating Akt-mediated phosphorylation of TSC2 (*red; third column*) and complete cytoplasmic localization of p27Kip1 (*green; fourth column*) in murine SmoA1 medulloblastoma are not altered by mTOR inhibition. All cells were costained with DAPI (*blue*). Magnification, ×63 (*first* and *second columns*) and ×120 (*third* and *fourth columns*). *C,* quantification of staining for the mitotic marker phosphorylated histone H3 in SmoA1 medulloblastoma treated with or without CCI-779 for 10 d. mTOR inhibition reduced levels of phosphorylated histone H3 (*, $P = 0.0052$). Two-tailed *t* tests were used to test significance. *D,* CCI-779 treatment reduces the levels of cell cycle regulators in SmoA1 tumor cells. SmoA1 medulloblastomas lose N-myc, cyclin D2, and vascular endothelial growth factor (*VEGF*) protein upon mTOR inhibition for 10 d. Wild-type mice were used as controls. *Bars, A* and *B* (*first* and *second columns*), 16 μm; *B* (*third* and *fourth columns*), 8 μm.

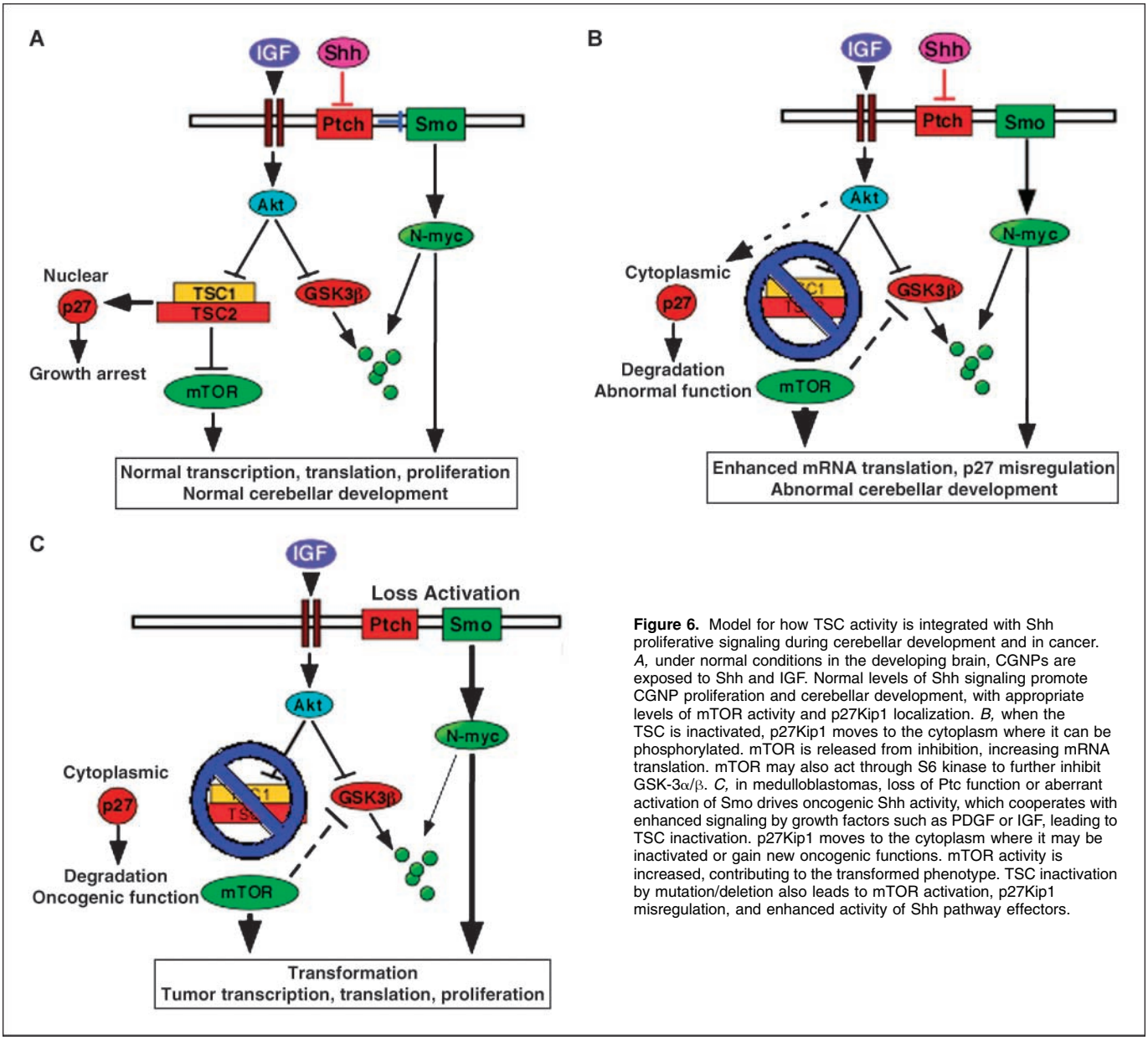

Figure 6. Model for how TSC activity is integrated with Shh proliferative signaling during cerebellar development and in cancer. *A,* under normal conditions in the developing brain, CGNPs are exposed to Shh and IGF. Normal levels of Shh signaling promote CGNP proliferation and cerebellar development, with appropriate levels of mTOR activity and p27Kip1 localization. *B,* when the TSC is inactivated, p27Kip1 moves to the cytoplasm where it can be phosphorylated. mTOR is released from inhibition, increasing mRNA translation. mTOR may also act through S6 kinase to further inhibit GSK-3α/β. *C,* in medulloblastomas, loss of Ptc function or aberrant activation of Smo drives oncogenic Shh activity, which cooperates with enhanced signaling by growth factors such as PDGF or IGF, leading to TSC inactivation. p27Kip1 moves to the cytoplasm where it may be inactivated or gain new oncogenic functions. mTOR activity is increased, contributing to the transformed phenotype. TSC inactivation by mutation/deletion also leads to mTOR activation, p27Kip1 misregulation, and enhanced activity of Shh pathway effectors.

decreases survival latency (Fig. 3*C*). Introducing the *TSC2-RGΔ* transgene increased phosphorylation of rpS6, GSK-3α/β, and $p27^{Kip1}$ (Fig. 3*D*) in the tumors. Taken together, these results suggest that Shh signaling and TSC inactivation could cooperate to enhance medulloblastoma formation.

TSC rescues $p27^{Kip1}$ localization and reduces the proliferation of Shh-mediated medulloblastoma cells. In order to determine whether TSC inactivation and $p27^{Kip1}$ dysregulation are related, we turned to a Shh-associated medulloblastoma cell line model, the Pzp53med cell line, derived from a $Ptc^{+/-}p53^{-/-}$ mouse medulloblastoma (38). Recently, the Scott group characterized Gli expression and sensitivity to sterol synthesis inhibitors in these cells (39). We found robust levels of phosphorylated rpS6 in Pzp53med cells (Fig. 4*A, left*). Consistent with mTOR activation lying downstream of Akt, which phosphorylates and inactivates TSC2 (13, 40), treatment of the Pzp53med cells with the phosphoinositide-3-kinase inhibitor wortmannin eliminated rpS6 phosphorylation (Fig. 4*A, middle*). Rapamycin treatment also eliminated rpS6 phosphorylation (Fig. 4*A, right*). Moreover, total TSC2 and $p27^{Kip1}$ levels were low (Fig. 4*B, left*) in the Pzp53med cells. Wortmannin treatment increased TSC2 protein levels and returned $p27^{Kip1}$ to the nucleus, whereas rapamycin did not, suggesting that TSC2 inactivation and $p27^{Kip1}$ stabilization are regulated upstream of mTOR (Fig. 4*B, middle* and *right*) in the Pzp53med cells, as in CGNPs. To determine whether $p27^{Kip1}$ localization was dependent on TSC in these cells, we introduced exogenous TSC2 by transient transfection. Cells expressing TSC2 had nuclear $p27^{Kip1}$ (Fig. 4*C, left* and *middle*). Indeed, nearly 90% of TSC2-positive cells had nuclear $p27^{Kip1}$, as compared with only 10% of TSC2-negative cells (Fig. 4*C, right*). These results suggest that low levels of TSC2 may be associated with increased $p27^{Kip1}$ turnover in the medulloblastoma cells. To determine whether reconstituting TSC

activity impedes cell cycle progression in Pzp53med cells, we coimmunostained for TSC2 and BrdUrd. We observed an inverse correlation between TSC2-positive cells and BrdUrd-positive cells: overexpression of TSC2 reduced proliferation by ~4-fold (Fig. 4*D*). Finally, TSC2 and $p27^{Kip1}$ were rapidly degraded in the cytoplasm of Pzp53 medulloblastoma cells (Fig. 4*B*; Supplementary Fig. S2, *left*). TSC2 accumulates in Pzp53med cells treated with the proteasome inhibitor lactacystin (Supplementary Fig. S2, *middle*), and its localization to the nucleus is associated with increased nuclear $p27^{Kip1}$ (Supplementary Fig. S2, *right*). Together, our results show that $p27^{Kip1}$ localization depends on TSC2 expression and function.

p27 is mislocalized in Shh-mediated medulloblastoma. We wished to determine whether mTOR inhibition affects tumor growth and p27 localization in *SmoA1* medulloblastoma *in vivo*. We treated wild-type adult mice with the mTOR inhibitor CCI-779 for 9 to 10 days (40 mg/kg daily) using i.p. injection of the drug. Data shown are representative of results from five treated mice and five untreated mice. Before treatment, phosphorylation of rpS6 was restricted to the Purkinje cells of normal adult cerebella. Following treatment, phosphorylated rpS6 was virtually undetectable (Fig. 5*A*). As shown in Fig. 3 and Fig. 5*A* and *B, SmoA1* medulloblastomas possessed Bmi1 (41, 42), a progenitor cell marker, and phosphorylated rpS6, indicating mTOR pathway activation. The phosphorylated rpS6 signal was not found in GFAP-positive cells (i.e., astrocytes) present in the tumor (Fig. 5*A*). Both phosphorylated GSK-3α/β and Akt-mediated phosphorylation of TSC2 were found in tumor cells (Fig. 5*B, top row*). Because we observe that TSC2 is phosphorylated on inactivating sites in *SmoA1* medulloblastomas, we asked whether $p27^{Kip1}$ was mislocalized in these tumors. As shown in Fig. 5*B* (*top row*), $p27^{Kip1}$ was found in the cytoplasm of the tumor cells. Indeed, no cells were observed with nuclear $p27^{Kip1}$. We also detected only cytoplasmic $p27^{Kip1}$ in $Ptc^{+/-}$ medulloblastomas (data not shown).

Recent reports (36, 43) have indicated that GSK-3α/β can be phosphorylated downstream of mTOR, and that $p27^{Kip1}$ localization can be regulated downstream of mTOR. Following CCI-779 treatment, rpS6 phosphorylation was eliminated in *NeuroD2-SmoA1* medulloblastomas (Fig. 5*B, bottom row*). GSK-3α/β phosphorylation was also down-regulated, suggesting that as in primary CGNPs (Figs. 2 and 3), GSK-3α/β phosphorylation is dependent on mTOR under TSC-inactive conditions (Fig. 5*B, bottom row*). The loss of GSK-3α/β phosphorylation was not due to the effects of CCI-779 on Akt, as TSC2 phosphorylation on the Akt-targeted site T1462 was not affected by CCI-779 treatment (Fig. 5*B, bottom row*). Lastly, CCI-779 treatment did not promote $p27^{Kip1}$ relocalization to the nucleus, indicating that in medulloblastomas, $p27^{Kip1}$ subcellular localization is regulated upstream of mTOR (Fig. 5*B, bottom row*). Quantification of histone H3 phosphorylation (Fig. 5*C*) revealed a significant reduction in proliferation in treated medulloblastomas, as did Western blotting for N-myc and cyclin D2 (Fig. 5*D*). We also observed decreased levels of vascular endothelial growth factor protein following CCI-779 treatment (Fig. 5*D*). Previous reports have shown that mTOR induces vascular endothelial growth factor production, which is vital for tumor growth through angiogenesis (44).

Discussion

Somatic mutations in TSC1 or TSC2 cause tuberous sclerosis (40, 45). Although patients with tuberous sclerosis themselves are not predisposed to develop medulloblastoma, the TSC can be inactivated by phosphorylation downstream of growth factors associated with medulloblastoma, such as PDGF and IGF, and a small study identified a point mutation in TSC2 in a subset of medulloblastomas (46). Here, we have asked whether loss of TSC activity may contribute to proliferation during normal cerebellar development and to the incidence or growth of medulloblastomas.

We found that mouse Shh-mediated medulloblastomas had high levels of mTOR activity, and biochemically resembled CGNPs derived from mice constitutively expressing a dominant negative TSC2 allele (*TSC2-RGΔ* mice). When we analyzed cerebellar development in these mice, we found that their CGNPs had an extended proliferative capacity *in vivo*, and *in vitro* they exhibited Shh-independent proliferation. When the *TSC2-RGΔ* allele was introduced into mice with aberrantly activated Shh signaling, the incidence of medulloblastoma was markedly increased, with reduced latency to tumor formation. These lines of evidence suggest that inactivation of the TSC complex could contribute to medulloblastoma formation, perhaps as a "second hit." Indeed, when we recently analyzed a human tumor collection for TSC-inactivating mutations, we identified TSC1 deletions in a significant number of tumors, and these tumors belonged to the Shh-associated subclass of medulloblastomas (Supplementary Fig. S3). The only known function of TSC1 is to stabilize TSC2 (47); therefore, loss of TSC1 in tumors results in the loss of TSC2 activity. We also explored the expression analysis of TSC2 and CDKN1B ($p27^{Kip1}$) in human Shh-subgroup medulloblastomas and found moderate decreases compared with adult cerebellum (Supplementary Fig. S4). TSC2 and p27 are not classic tumor suppressors, as they are rarely mutated or deleted in cancer, but they are often deregulated in cancer by post-translational modifications, as supported by our study and previous reports (48–50).

Interestingly, in the *TSC2-RGΔ* cerebellar EGL and *NeuroD2-SmoA1* medulloblastomas, we observed $p27^{Kip1}$ in the cytosol in all cells, associated with increased levels of phosphorylation on Ser10. Phosphorylation on $p27^{Kip1}$ Ser10 leads to its nuclear export and increased stability in the cytosol (34). When we transfected Pzp53med cells with exogenous TSC2, we found nuclear $p27^{kip1}$ in nearly 90% of TSC2-positive cells. A correlation between poor prognosis and cytoplasmic localization of $p27^{Kip1}$ in human tumors has led to the hypothesis that $p27^{Kip1}$ has an active tumor-promoting function in the cytoplasm (50). A recent study tested for CDK-independent functions of $p27^{Kip1}$ by analyzing knock-in mice expressing a mutant *p27* ($p27^{CK-}$) that is unable to inhibit cyclin-CDK complexes (25). These mice developed various tumors, and the $p27^{CK-}$ mutant localizes to the cytoplasm, hinting that a cytoplasmic function might mediate the oncogenic effects of $p27^{Kip1}$.

Taken together, our findings suggest the model shown in Fig. 6. Under normal developmental conditions, TSC modulates mTOR signaling, and stabilizes $p27^{Kip1}$ (Fig. 6*A*). Under conditions of TSC loss (Fig. 6*B*), mTOR activity is increased, $p27^{Kip1}$ is localized to the cytoplasm where it may be degraded, inactivated, or gain abnormal functions, and GSK-3α/β is phosphorylated (43), thus increasing N-myc protein levels and CGNP proliferation. In the setting of Shh-induced medulloblastoma (Fig. 6*C*), signaling by growth factors such as PDGF (9) or IGF could lead to TSC inactivation via phosphorylation by Akt or Erk2; alternatively, the TSC can be disrupted by mutation. Signaling by mTOR is activated, leading to increased translation of growth-associated

proteins and potential inhibition of GSK-3α/β. These factors can all contribute to enhanced tumor growth or decreased latency.

Development of hedgehog pathway inhibitors such as cyclopamine and HhAntag (51) has raised the hope that targeting this pathway will be an effective antimedulloblastoma strategy (51, 52). However, it has recently been shown that systemic treatment of young animals with hedgehog pathway inhibitors results in devastating, irreversible effects on bone growth (53). Gli1-transformed epithelioid cells require mTOR activity for their survival (54). Our observation that the mTOR pathway is activated in mouse and human medulloblastomas suggests that inhibitors of this pathway may be useful. Moreover, our demonstration that modulation of mTOR is not the only tumor-suppressive function of the TSC in the developing brain and in brain tumors suggests that using drugs to block the activation of TSC2-inhibiting pathways, or that can promote $p27^{Kip1}$ nuclear localization, may present even more effective future medulloblastoma therapies.

Disclosure of Potential Conflicts of Interest

No potential conflicts of interest were disclosed.

Acknowledgments

Received 4/7/09; revised 6/16/09; accepted 6/27/09; published OnlineFirst 9/8/09.

Grant support: The American Brain Tumor Association (B. Bhatia, in memory of Davis Ferguson), the National Institute of Neurological Disorders and Stroke (R01NS061070, A.M. Kenney), Children's Brain Tumor Foundation (A.M. Kenney), the Childhood Brain Tumor Foundation of Maryland (A.M. Kenney), the Pediatric Brain Tumor Foundation (A.M. Kenney), the Sontag Foundation (A.M. Kenney and M.D. Taylor), and the Brain Tumor Center of Memorial Sloan-Kettering Cancer Center (B. Bhatia).

The costs of publication of this article were defrayed in part by the payment of page charges. This article must therefore be hereby marked *advertisement* in accordance with 18 U.S.C. Section 1734 solely to indicate this fact.

We thank Jeffrey Miller, Ph.D., Andy Koff, Ph.D., Andrej Dlugosz, Ph.D., and Timothy Gershon, M.D., Ph.D. for their advice, helpful discussion, and expertise.

References

1. Rubin JB, Rowitch DH. Medulloblastoma: a problem of developmental biology. Cancer Cell 2002;2:7–8.
2. Knoepfler PS, Kenney AM. Neural precursor cycling at sonic speed: N-Myc pedals, GSK-3 brakes. Cell Cycle 2006;5:47–52.
3. Wetmore C. Sonic hedgehog in normal and neoplastic proliferation: insight gained from human tumors and animal models. Curr Opin Genet Dev 2003;13:34–42.
4. Pietsch T, Waha A, Koch A, et al. Medulloblastomas of the desmoplastic variant carry mutations of the human homologue of Drosophila patched. Cancer Res 1997;57:2085–8.
5. Raffel C, Jenkins RB, Frederick L, et al. Sporadic medulloblastomas contain PTCH mutations. Cancer Res 1997;57:842–5.
6. Wang JY, Del Valle L, Gordon J, et al. Activation of the IGF-IR system contributes to malignant growth of human and mouse medulloblastomas. Oncogene 2001;20:3857–68.
7. Hartmann W, Koch A, Brune H, et al. Insulin-like growth factor II is involved in the proliferation control of medulloblastoma and its cerebellar precursor cells. Am J Pathol 2005;166:1153–62.
8. Inoki K, Corradetti MN, Guan KL. Dysregulation of the TSC-mTOR pathway in human disease. Nat Genet 2005;37:19–24.
9. Gilbertson RJ, Clifford SC. PDGFRB is overexpressed in metastatic medulloblastoma. Nat Genet 2003;35:197–8.
10. Soucek T, Pusch O, Wienecke R, DeClue JE, Hengstschlager M. Role of the tuberous sclerosis gene-2 product in cell cycle control. Loss of the tuberous sclerosis gene-2 induces quiescent cells to enter S phase. J Biol Chem 1997;272:29301–8.
11. Soucek T, Rosner M, Miloloza A, et al. Tuberous sclerosis causing mutants of the TSC2 gene product affect proliferation and p27 expression. Oncogene 2001;20:4904–9.
12. Rosner M, Hengstschlager M. Tuberin binds p27 and negatively regulates its interaction with the SCF component Skp2. J Biol Chem 2004;279:48707–15.
13. Rosner M, Freilinger A, Hanneder M, et al. p27Kip1 localization depends on the tumor suppressor protein tuberin. Hum Mol Genet 2007;16:1541–56.
14. Miyazawa K, Himi T, Garcia V, Yamagishi H, Sato S, Ishizaki Y. A role for p27/Kip1 in the control of cerebellar granule cell precursor proliferation. J Neurosci 2000;20:5756–63.
15. Shambaugh GE 3rd, Haines GK 3rd, Koch A, Lee EJ, Zhou J, Pestell R. Immunohistochemical examination of the INK4 and Cip inhibitors in the rat neonatal cerebellum: cellular localization and the impact of protein calorie malnutrition. Brain Res 2000;855:11–22.
16. Ayrault O, Zindy F, Rehg J, Sherr CJ, Roussel MF. Two tumor suppressors, p27Kip1 and patched-1, collaborate to prevent medulloblastoma. Mol Cancer Res 2009;7:33–40.
17. Zindy F, Knoepfler PS, Xie S, Sherr CJ, Eisenman RN, Roussel MF. N-Myc and the cyclin-dependent kinase inhibitors p18Ink4c and p27Kip1 coordinately regulate cerebellar development. Proc Natl Acad Sci U S A 2006;103:11579–83.
18. Knoepfler PS, Cheng PF, Eisenman RN. N-myc is essential during neurogenesis for the rapid expansion of progenitor cell populations and the inhibition of neuronal differentiation. Genes Dev 2002;16:2699–712.
19. Diehl JA, Cheng M, Roussel MF, Sherr CJ. Glycogen synthase kinase-3β regulates cyclin D1 proteolysis and subcellular localization. Genes Dev 1998;12:3499–511.
20. Govindarajan B, Brat DJ, Csete M, et al. Transgenic expression of dominant negative tuberin through a strong constitutive promoter results in a tissue-specific tuberous sclerosis phenotype in the skin and brain. J Biol Chem 2005;280:5870–4.
21. Kenney AM, Widlund HR, Rowitch DH. Hedgehog and PI-3 kinase signaling converge on Nmyc1 to promote cell cycle progression in cerebellar neuronal precursors. Development 2004;131:217–28.
22. Kwiatkowski DJ, Zhang H, Bandura JL, et al. A mouse model of TSC1 reveals sex-dependent lethality from liver hemangiomas, and up-regulation of p70S6 kinase activity in Tsc1 null cells. Hum Mol Genet 2002;11:525–34.
23. Uziel T, Zindy F, Xie S, et al. The tumor suppressors Ink4c and p53 collaborate independently with Patched to suppress medulloblastoma formation. Genes Dev 2005;19:2656–67.
24. Shakhova O, Leung C, van Montfort E, Berns A, Marino S. Lack of Rb and p53 delays cerebellar development and predisposes to large cell anaplastic medulloblastoma through amplification of N-Myc and Ptch2. Cancer Res 2006;66:5190–200.
25. Besson A, Hwang HC, Cicero S, et al. Discovery of an oncogenic activity in p27Kip1 that causes stem cell expansion and a multiple tumor phenotype. Genes Dev 2007;21:1731–46.
26. Besson A, Gurian-West M, Chen X, Kelly-Spratt KS, Kemp CJ, Roberts JM. A pathway in quiescent cells that controls p27Kip1 stability, subcellular localization, and tumor suppression. Genes Dev 2006;20:47–64.
27. Sicinski P, Zacharek S, Kim C. Duality of p27Kip1 function in tumorigenesis. Genes Dev 2007;21:1703–6.
28. Ciemerych MA, Kenney AM, Sicinska E, et al. Development of mice expressing a single D-type cyclin. Genes Dev 2002;16:3277–89.
29. Dahmane N, Ruiz i Altaba A. Sonic hedgehog regulates the growth and patterning of the cerebellum. Development 1999;126:3089–100.
30. Wallace VA. Purkinje-cell-derived Sonic hedgehog regulates granule neuron precursor cell proliferation in the developing mouse cerebellum. Curr Biol 1999;9:445–8.
31. Wechsler-Reya RJ, Scott MP. Control of neuronal precursor proliferation in the cerebellum by Sonic Hedgehog. Neuron 1999;22:103–14.
32. Dudek H, Datta SR, Franke TF, et al. Regulation of neuronal survival by the serine-threonine protein kinase Akt. Science (New York, NY) 1997;275:661–5.
33. Miller TM, Tansey MG, Johnson EM, Jr., Creedon DJ. Inhibition of phosphatidylinositol 3-kinase activity blocks depolarization- and insulin-like growth factor I-mediated survival of cerebellar granule cells. J Biol Chem 1997;272:9847–53.
34. Rodier G, Montagnoli A, Di Marcotullio L, et al. p27 cytoplasmic localization is regulated by phosphorylation on Ser10 and is not a prerequisite for its proteolysis. EMBO J 2001;20:6672–82.
35. Ishida N, Hara T, Kamura T, Yoshida M, Nakayama K, Nakayama KI. Phosphorylation of p27Kip1 on serine 10 is required for its binding to CRM1 and nuclear export. J Biol Chem 2002;277:14355–8.
36. Hong F, Larrea MD, Doughty C, Kwiatkowski DJ, Squillace R, Slingerland JM. mTOR-raptor binds and activates SGK1 to regulate p27 phosphorylation. Mol Cell 2008;30:701–11.
37. Hallahan AR, Pritchard JI, Hansen S, et al. The SmoA1 mouse model reveals that notch signaling is critical for the growth and survival of sonic hedgehog-induced medulloblastomas. Cancer Res 2004;64:7794–800.
38. Berman DM, Karhadkar SS, Hallahan AR, et al. Medulloblastoma growth inhibition by hedgehog pathway blockade. Science 2002;297:1559–61.
39. Corcoran RB, Scott MP. Oxysterols stimulate Sonic hedgehog signal transduction and proliferation of medulloblastoma cells. Proc Natl Acad Sci U S A 2006;103:8408–13.
40. Astrinidis A, Henske EP. Tuberous sclerosis complex: linking growth and energy signaling pathways with human disease. Oncogene 2005;24:7475–81.
41. Michael LE, Westerman BA, Ermilov AN, et al. Bmi1 is required for Hedgehog pathway-driven medulloblastoma expansion. Neoplasia 2008;10:1343–9, 5p following 9.
42. Leung C, Lingbeek M, Shakhova O, et al. Bmi1 is essential for cerebellar development and is overexpressed in human medulloblastomas. Nature 2004;428:337–41.
43. Zhang HH, Lipovsky AI, Dibble CC, Sahin M, Manning BD. S6K1 regulates GSK3 under conditions of mTOR-dependent feedback inhibition of Akt. Mol Cell 2006;24:185–97.
44. El-Hashemite N, Walker V, Zhang H, Kwiatkowski DJ. Loss of Tsc1 or Tsc2 induces vascular endothelial

growth factor production through mammalian target of rapamycin. Cancer Res 2003;63:5173–7.
45. Crino PB, Nathanson KL, Henske EP. The tuberous sclerosis complex. N Engl J Med 2006; 355:1345–56.
46. Przkora R, Meyer-Puttlitz B, Schmitt O, et al. Analysis of the TSC2 gene in human medulloblastoma. Acta Neuropathol 2001;102:380–4.
47. Chong-Kopera H, Inoki K, Li Y, et al. TSC1 stabilizes TSC2 by inhibiting the interaction between TSC2 and the HERC1 ubiquitin ligase. J Biol Chem 2006;281: 8313–6.
48. Kwiatkowski DJ, Manning BD. Tuberous sclerosis: a GAP at the crossroads of multiple signaling pathways. Hum Mol Genet 2005;14 Spec No. 2:R251–8.
49. Chu IM, Hengst L, Slingerland JM. The Cdk inhibitor p27 in human cancer: prognostic potential and relevance to anticancer therapy. Nat Rev Cancer 2008;8:253–67.
50. Slingerland J, Pagano M. Regulation of the cdk inhibitor p27 and its deregulation in cancer. J Cell Physiol 2000;183:10–7.
51. Romer J, Curran T. Targeting medulloblastoma: small-molecule inhibitors of the Sonic Hedgehog pathway as potential cancer therapeutics. Cancer Res 2005;65:4975–8.
52. Stecca B, Ruiz i Altaba A. The therapeutic potential of modulators of the Hedgehog-Gli signaling pathway. J Biol 2002;1:9.
53. Kimura H, Ng JM, Curran T. Transient inhibition of the Hedgehog pathway in young mice causes permanent defects in bone structure. Cancer Cell 2008;13:249–60.
54. Louro ID, McKie-Bell P, Gosnell H, Brindley BC, Bucy RP, Ruppert JM. The zinc finger protein GLI induces cellular sensitivity to the mTOR inhibitor rapamycin. Cell Growth Differ 1999;10:503–16.